Circulation in Quasi-2D Turbulence: Experimental Observation of the Area Rule and Bifractality

Hang-Yu Zhu (朱航宇)[1], Jin-Han Xie (谢金翰)[2], and Ke-Qing Xia (夏克青)[1,3,*]

[1]*Center for Complex Flows and Soft Matter Research and Department of Mechanics and Aerospace Engineering, Southern University of Science and Technology, Shenzhen 518055, China*

[2]*Department of Mechanics and Engineering Science at College of Engineering, and State Key Laboratory for Turbulence and Complex Systems, Peking University, Beijing 100871, China*

[3]*Department of Physics, Southern University of Science and Technology, Shenzhen 518055, China*

We present an experimental study of the velocity circulation in a quasi-two-dimensional turbulent flow. We show that the area rule of circulation around simple loops holds in both the forward cascade enstrophy inertial range (ΩIR) and the inverse cascade energy inertial range (EIR): When the side lengths of a loop are all within the same inertial range, the circulation statistics depend on the loop area alone. It is also found that, for circulation around figure-eight loops, the area rule still holds in EIR but is not applicable in ΩIR. In ΩIR, the circulation is nonintermittent; whereas in EIR, the circulation is bifractal: space filling for moments of the order of 3 and below and a monofractal with a dimension of 1.42 for higher orders. Our results demonstrate, as in a numerical study of 3D turbulence [K. P. Iyer et al., Circulation in High Reynolds Number Isotropic Turbulence is a Bifractal, Phys. Rev. X **9**, 041006 (2019).], that, in terms of circulation, turbulent flows exhibit a simpler behavior than velocity increments, as the latter are multifractals.

A major issue in the study of turbulence is to find its putatively universal small-scale properties. Most existing theories of turbulence based on phenomenology and mathematical analysis largely focus on the structure function (SF) $\langle |\delta u_r|^p \rangle$ (δu_r is the velocity increment over a distance r), as their scaling laws can characterize the dynamics of energy cascade [1]. The celebrated K41 theory [2] predicted that, in the inertial range (IR) of three-dimensional (3D) turbulence, the velocity SFs scale as $\langle |\delta u_r|^p \rangle \propto r^{p/3}$. However, later studies [3–5] found that, due to the intermittency effect, the scalings exhibit multifractality (i.e., a nonlinear function of moment order), which is difficult to understand analytically. This problem is further aggravated, as high-order longitudinal and transverse SFs scale differently [6–8]. This difficulty motivates the community to seek other theoretical metrics that may be used to describe turbulence in a simpler way. A recent numerical study of high Taylor-scale Reynolds number (Re$_\lambda$) 3D turbulence [9] suggests that the circulation $\Gamma_A = \oint_C \boldsymbol{u} \cdot d\boldsymbol{l}$ (A is the area enclosed by the loop C and $d\boldsymbol{l}$ is the line element along C) may be such an object, which is simpler than velocity itself: Circulation in IR is bifractal and satisfies the area rule [10,11].

Circulation was also found numerically to be a bifractal in quantum turbulence [12,13] despite the distinct difference of vortex distributions in quantum and classical turbulence [14,15], which connects the intermittency in the two types of turbulence [1,16]. In addition, recent experiments in two-dimensional (2D) quantum turbulence [17–19] observed the coherent vortex dynamics and condensates, as in classical 2D turbulence [20,21]. Classical 2D turbulence is also closely related to physical processes for large-scale motions in geophysical flows [22]. There exist essential differences between 2D and 3D turbulence, such as the conserved quantities, the direction of energy transfer [20], and the degree of intermittency in terms of velocity SFs [22,23], which hinder the establishment of a unified theory of turbulence. It is, thus, highly desirable to find a single physical quantity that has the same (or similar) characteristics in both 2D and 3D turbulence, which, in turn, may afford us a more universal description of turbulence.

The bifractality and area rule have not been observed experimentally so far, in both 3D and 2D turbulence. In the case of low-Re$_\lambda$ 3D turbulence with insufficient extent of IR, previous simulations and experiments have not been able to verify the applicability of the area rule, and it was suggested that the circulation was also multifractal as the velocity increments [24–27], in contrast with the findings in high-Re$_\lambda$ turbulence [9]. Moreover, the study of circulation in 2D turbulence is made more interesting by its two IRs for energy and enstrophy cascades.

In this Letter, the circulation properties in a quasi-2D turbulent flow are studied experimentally. We show that, in the energy inertial range (EIR) of 2D turbulence, circulation possesses bifractality, as in 3D and quantum

turbulence; whereas in the enstrophy inertial range (ΩIR), circulation is nonintermittent. We also show that the area rule for circulation around simple loops holds in both EIR and ΩIR.

Our 2D turbulence was generated electromagnetically in stratified thin fluid layers. The experimental setup (see Supplemental Material [28]) is similar to those described in Refs. [21,39,40]. A conducting fluid of NaOH water solution (density 1.08 g/cm^3) is floated on a heavier, immiscible, dielectric fluid layer, FC-770 (density 1.79 g/cm^3). A direct current is driven through the top layer with two copper electrodes at each end of the reservoir. Beneath the reservoir is a square matrix of 30×30 neodymium-iron-boron (NdFeB) grade N52 magnets. Each magnet is $10 \times 10 \times 5$ mm^3 and has a peak magnetic field of about 0.43 T. The magnets are placed 10 mm apart (which gives rise to the forcing scale l_f) in a checkerboard pattern with the poles of adjacent magnets arranged oppositely, which has the advantage of driving stronger fluctuating kinetic energy and facilitating the inverse energy transfer [41]. The resulting Lorenz forces from the interaction between the current and the vertical magnetic field generate a vortex lattice in the top fluid that evolves to turbulent flows.

The flow fields were measured by particle image velocimetry. The top fluid layer was seeded with 50 μm polyamide spheres and illuminated by a horizontal laser sheet. A high-resolution camera (3000×3000 pixels^2, at 40 frames per second) recorded 7221 realizations of flow field in the steady state. The spatial resolution l_{res} of the measured velocity field is 0.52 mm, and the measurement domain L is 193×193 mm^2, resulting in $l_f/l_{res} = 19.2$ and $L/l_f = 19.3$. The entire flow region L_B is 300×300 mm^2, i.e., $L_B/l_f = 30$, so little boundary effect of the sidewalls on the flow in the measurement domain can be expected. We have close to 10^9 ($371 \times 371 \times 7221$) measured velocity vectors, which ensures the convergence of high-order velocity and circulation SFs. The Reynolds number Re$_f$ based on l_f and u_{rms} is 110, and Re$_\lambda$ is 60. This is a typical value where turbulent flow is generally considered to be fully developed and simultaneously the 3D effect is negligible [40,42].

It is challenging for experiments to simultaneously observe both IRs with sufficient extent in 2D turbulence [39,43,44]. To do so, sufficient scale separations are required, i.e., $l_f/l_\nu \gg 1$ and $L_\alpha/l_f \gg 1$ [22], where l_ν is the viscous scale and L_α the friction-dominated scale. In this experiment, we have $L_\alpha/l_f = 13.7$ and $l_f/l_\nu = 12.5$, so the above conditions are well satisfied. Verification of the two-dimensionality of the flow and the existence of the two IRs are presented in Supplemental Material [28]. From the second-order circulation moment, as shown later, we can estimate the extent of the IRs, i.e., ΩIR: $0.05 < r/l_f < 0.7$; EIR: $1.0 < r/l_f < 6.0$.

With the measured velocity field, we calculate the SFs of velocity $\langle |\delta u_r|^p \rangle$ and circulation $\langle |\Gamma_A|^p \rangle$. For 2D, the
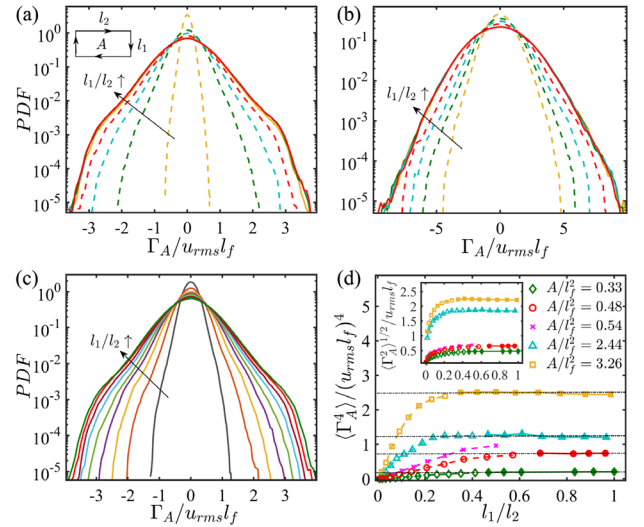

FIG. 1. PDF of Γ_A for loops with different l_1/l_2 and fixed area $A/l_f^2 = 0.48$ (a), 2.44 (b), and 0.54 (c). (d) $\langle \Gamma_A^4 \rangle$ and $\langle \Gamma_A^2 \rangle^{1/2}$ (inset) versus l_1/l_2 (the vertical scale for $A/l_f^2 = 2.44$, 3.26 is reduced by 30 times in the main figure). In (a), (b), and (d), the dashed lines and hollow symbols denote loops with at least one side outside ΩIR (for $A/l_f^2 = 0.33$ or 0.48) or EIR (for $A/l_f^2 = 2.44$ or 3.26), and the solid lines and symbols indicate both sides of loops are inside the same IR. All curves in (c) and the crosses in (d) represent the loops with l_1 inside ΩIR and l_2 inside EIR.

minimal area is no different from the classical area. Figure 1(a) plots the probability density functions (PDFs) of Γ_A normalized by $u_{rms}l_f$ for several rectangular loops with the same loop area ($A/l_f^2 = 0.48$) but different aspect ratios (l_1/l_2). One sees that, when the lengths of both sides of the loop are contained within the ΩIR, the corresponding PDFs collapse to a very good accuracy; whereas, with one of the lengths outside ΩIR, the PDFs manifest an aspect-ratio dependence. This indicates that the area rule holds in ΩIR. Likewise, the area rule is also applicable in EIR [Fig. 1(b)]: When both sides of the loop are within EIR, the PDFs of Γ_A are independent of l_1/l_2. Also, when l_1 lies in ΩIR and l_2 is within EIR, respectively, the PDFs present a noticeable dependence on l_1/l_2; see Fig. 1(c) and the crosses in Fig. 1(d). It indicates that the area rule is not valid unless both sides are within the same IR. Figure 1(d) plots the second- and fourth-order moments of circulation versus l_1/l_2 for two values of A/l_f^2 in each IR. It shows that the circulation satisfies the area rule at least to a fourth-order accuracy in both IRs in our quasi-2D turbulence.

The above findings support the previous theoretical and numerical studies on the area rule [9–11,45]. Furthermore, our results suggest that the area rule of circulation works not only in EIR for forward cascade, but also in EIR for inverse cascade and ΩIR for forward cascade. It suggests that, in terms of area rule, the circulation statistics are more universal and may serve as a unifying quantity for both 2D and 3D turbulence.
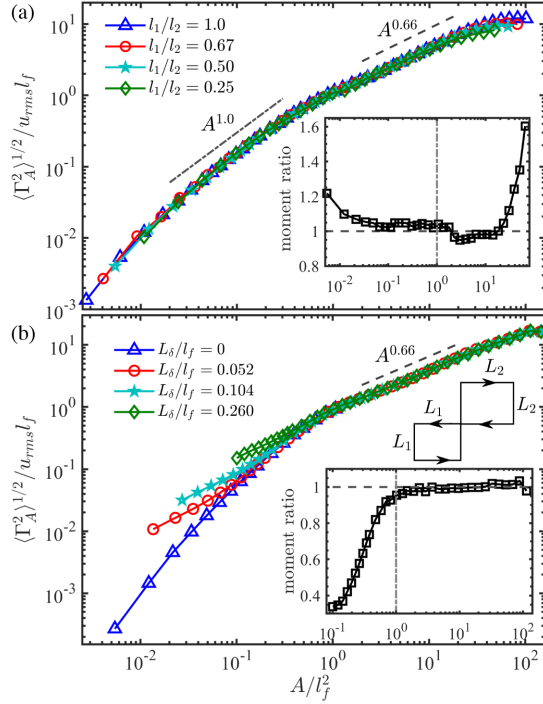
FIG. 2. $\langle \Gamma_A^2 \rangle^{1/2}$ versus A for four sets of (a) simple loops and (b) figure-eight loops. The inset in (a) plots the ratio of $\langle \Gamma_A^2 \rangle^{1/2}$ for $l_1/l_2 = 1$ to that for $l_1/l_2 = 0.5$. The inset in (b) plots the ratio of $\langle \Gamma_A^2 \rangle^{1/2}$ for $L_\delta/l_f = 0.104$ to that for $L_\delta/l_f = 0.260$.

We now investigate the effect of loop shape on the scaling of circulation SFs to quantify the applicability and limitations of the area rule in a wide range of scales. Figure 2(a) plots $\langle \Gamma_A^2 \rangle^{1/2}$ versus A/l_f^2 for four sets of rectangular loops with different l_1/l_2. One sees that $\langle \Gamma_A^2 \rangle^{1/2}$ is nearly independent of l_1/l_2 over a wide range of scales in both EIR and ΩIR ($0.01 \lesssim A/l_f^2 \lesssim 30$) for loops with rectangular shape, i.e., simple loops [inset in Fig. 2(a)]. The variation of $\langle \Gamma_A^2 \rangle^{1/2}$ with l_1/l_2 observed for small areas ($A/l_f^2 \lesssim 0.01$) may result from the viscous effect or small-scale three-dimensional flow effect [39,40,46,47], while for large areas ($A/l_f^2 \gtrsim 30$) it may be attributed to finite sampling [9]. Nevertheless, one sees that the area rule holds for simple loops to an excellent degree in both IRs.

Figure 2(b) plots the normalized $\langle \Gamma_A^2 \rangle^{1/2}$ versus A/l_f^2 for four sets of figure-eight loops of different shapes. This type of loop consists of two squares sharing a vertex, and its size can be characterized by the scalar area A ($= L_1^2 + L_2^2$) and its shape by L_δ ($= |L_1 - L_2|$). It is seen that $\langle \Gamma_A^2 \rangle^{1/2}$ is independent of L_δ/l_f for $A/l_f^2 \geq 1$ [inset in Fig. 2(b)]. This suggests that the area rule also holds for the more complicated loops in EIR, whereas in ΩIR $\langle \Gamma_A^2 \rangle^{1/2}$ decreases with decreasing L_δ. Note that turbulent flows in our system arise from the evolution of vortex lattice generated by the array of magnets, and a typical vortex size is of the order of $O(l_f)$. Therefore, when the size of a

figure-eight loop is comparable with or smaller than the size of a vortex, the subloops have opposite contributions to the circulation. It is this cancellation that results in a smaller value of circulation for small L_δ. Because of this, when discussing the scaling exponents of the circulation SFs below, we will consider only the simple square loops ($l_1/l_2 = 1$). There is thus no ambiguity when we speak of Γ_r, because $r = A^{1/2}$.

From dimensional analysis, the scaling exponents of circulation and velocity SFs should satisfy $\zeta_p = \chi_p + p$, where $\langle |\Gamma_r|^p \rangle \propto r^{\zeta_p}$ and $\langle |\delta u_r|^p \rangle \propto r^{\chi_p}$. According to K41 arguments [2], for $p = 1$, $\langle \Gamma_A^2 \rangle^{1/2}$ in ΩIR should scale as $\langle \Gamma_A^2 \rangle^{1/2} \propto r^2 \propto A^1$ ($\delta u_r \propto r^1$), while in EIR $\langle \Gamma_A^2 \rangle^{1/2} \propto r^{4/3} \propto A^{2/3}$ ($\delta u_r \propto r^{1/3}$). Both scalings are clearly verified in Fig. 2(a) for circulation around simple loops. As for the figure-eight loops, one can also observe $\langle \Gamma_A^2 \rangle^{1/2} \propto A^{2/3}$ in EIR. It indicates that the statistically relevant area for the circulation in EIR is the scalar area enclosed by the figure-eight loop, consistent with a previous study in 3D turbulence [9].

Figures 3(a) and 3(b) plot the circulation SFs of orders 1–10 and their local scaling exponents. One sees that, below l_f, ζ_p varies with r/l_f and a scaling range with a constant ζ_p is not observed, whereas, in the range of $2 \leq r/l_f \leq 6$, ζ_p are nearly invariant. In Fig. 3(b), a valley (indicated by the gray arrow) is seen (especially for high orders), and it may be understood as a result of the cancellation of circulation contributions from the counter-rotating vortex pairs in loops with size $\sim 2l_f$ [see the cartoon in Fig. 3(b)]. Therefore, we obtain the absolute scaling exponents $\zeta_{p,E}$ in the range of $2 \leq r/l_f \leq 6$ for EIR and the relative scaling exponents $\zeta_{p,\Omega}/\zeta_{2,\Omega}$ in ΩIR using the extended self-similarity (ESS) approach [48]. Integral
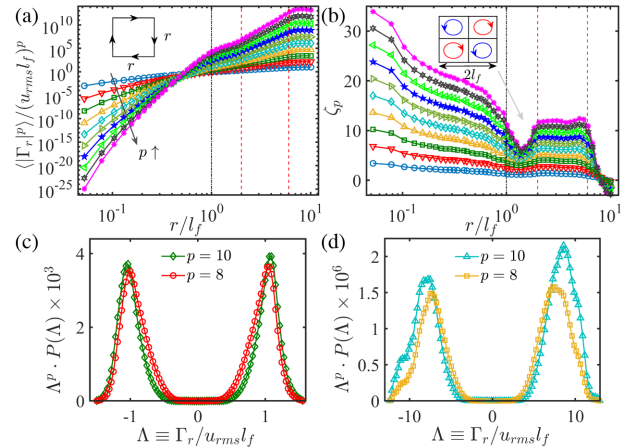

FIG. 3. (a) Circulation SFs of orders 1–10 and (b) corresponding local scaling exponents ζ_p as functions of r/l_f. Also shown are the integral kernels of circulation moments [$\langle \Lambda^p \rangle = \int \mathrm{PDF}(\Lambda) \Lambda^p d\Lambda$] at (c) $r/l_f = 0.4$ in ΩIR and (d) $r/l_f = 2.2$ in EIR for $p = 10$ and 8 [the vertical scale for $p = 8$ in (d) is enlarged by 50 times].
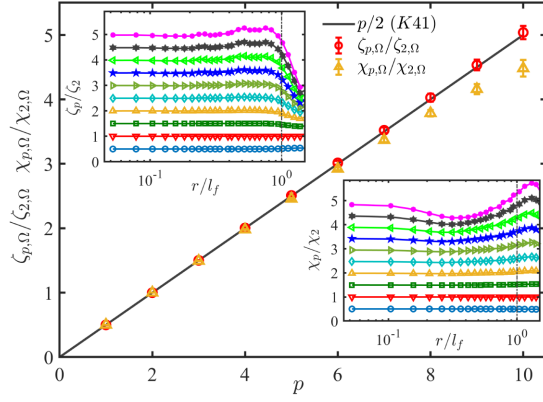
FIG. 4. The relative scaling exponents for $\langle|\Gamma_r|^p\rangle$ and $\langle|\delta u_r|^p\rangle$ within $0.05 < r/l_f < 0.7$. The insets plot, respectively, ζ_p/ζ_2 and χ_p/χ_2 versus r/l_f for $p = 1$–10 (from bottom to top).

kernels in Figs. 3(c) and 3(d) show the high level of convergence of high-order circulation SFs in the two IRs. We similarly obtain the (relative) scaling exponents χ_p of velocity SFs.

Figure 4 plots the exponents of velocity and circulation SFs in ΩIR versus p. The linear relation $\zeta_{p,\Omega}/\zeta_{2,\Omega} = p/2$ clearly indicates that the circulation is nonintermittent. However, the velocity increments in ΩIR seem to be weakly intermittent, although the deviation from the linear relation $\chi_{p,\Omega}/\chi_{2,\Omega} = p/2$ becomes apparent only for $p \geq 6$. This finding is consistent with results from a previous study [39] that showed the relation $\chi_{p,\Omega}/\chi_{2,\Omega} = p/2$ was roughly satisfied for $p \leq 6$. Note that the deviation for high orders may also originate from the logarithmic corrections [22,49].

The scaling behaviors for the circulation and velocity SFs in EIR are distinctly different from those in ΩIR. For the circulation SFs, Fig. 5(a) shows that $\zeta_{p,E}$ starts to deviate from K41 predictions for $p > 3$, indicating the presence of intermittency. It is interesting that $\zeta_{p,E}$ for $p > 3$ can be fitted with a linear relation: $\zeta_{p,E} = hp + (2 - D_2)$, where $h = 1.14 \pm 0.02$ and the Hölder dimension $D_2 = 1.42$. This suggests that the velocity circulation in EIR of our quasi-2D turbulent flow is a bifractal. In previous numerical studies of high-Re 3D turbulence [9] and quantum turbulence [12], circulation was also found to possess bifractality: a space-filling quantity for orders $p \leq 3$ and a monofractal with a Hölder dimension of 2.2 for orders $p > 3$ [inset in Fig. 5(a)]. The authors in Ref. [9] inferred that the monofractal dimension for high orders was due to moderately wrinkled vortex sheets rather than more complex singularities. Following the arguments in Ref. [1], the probability of the extreme events of circulation (i.e., the manifestation of intermittency) has a scaling of $\mathcal{P}(\Gamma_r) \propto (r/r_0)^{d-D}$, where d is the dimension of the embedding space, D the fractal dimension, and r_0 the integral length scale of turbulence. From dimensional analysis, the energy flux can be expressed as $\epsilon \propto \Gamma_r^3 r^{-4} \mathcal{P}(\Gamma_r)$. In 2D turbulence,
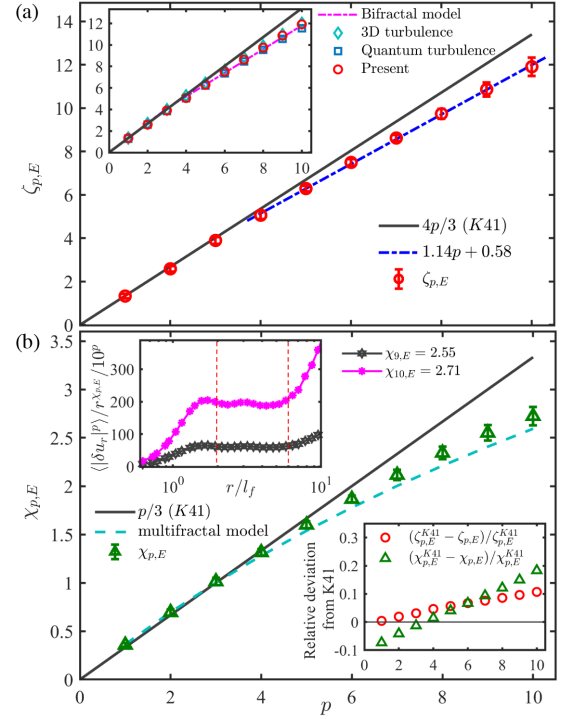

FIG. 5. The scaling exponents for (a) $\langle|\Gamma_r|^p\rangle$ and (b) $\langle|\delta u_r|^p\rangle$ in EIR. In (a), the high orders can be fitted by a monofractal model: $\zeta_{p,E} = 1.14p + 0.58$. Its inset displays bifractality observed in 3D turbulence [9], quantum turbulence [12], and present quasi-2D turbulence, and the magenta line denotes the bifractal model from Ref. [9]. In (b), the dashed line denotes the multifractal model for 3D turbulence [50,51]. The upper inset plots the compensated $\langle|\delta u_r|^p\rangle$ for $p = 9$ and 10 to show the scaling range, and the lower inset compares the relative deviations of $\zeta_{p,E}$ and $\chi_{p,E}$ from their respective K41 estimates.

it is a constant and independent of the scales in EIR. This implies $\Gamma_r \propto r^h$, and the circulation SFs scale as $\langle\Gamma_r^p\rangle \propto \Gamma_r^p \mathcal{P}(\Gamma_r) \propto r^{\zeta_p}$ with $\zeta_p = hp + (d - D)$ and $3h + (d - D) = 4$. The fitting result in Fig. 5(a) for $p > 3$ is perfectly consistent with the above theoretical argument, i.e., $3h + (d - D_2) = 4.0$, with $h = 1.14$, $d = 2$, and $D_2 = 1.42$.

Figure 5(b) plots $\chi_{p,E}$ for velocity SFs in EIR. One sees that δu_r exhibits a close-to-multifractal behavior. This contrasts with previous numerical results for 2D turbulence in which δu_r in EIR was nonintermittent [52] but agrees to some degree with those from earlier quasi-2D experiments [23,39,53,54]. It should be noted that our results are based on the absolute scaling exponents for orders up to 10, whereas in the earlier experiments the relative exponents using ESS were reported due to the lack of a clear scaling for $\langle|\delta u_r|^p\rangle$. As for the origin of intermittency in our quasi-2D turbulence, it may be attributed to the thin-layer effect, i.e., the imperfect two-dimensionality, and the presence of coherent structures.

In summary, we have shown for the first time experimentally in a quasi-2D turbulence that the statistical

moments of circulation exhibit bifractal behavior in EIR, whereas the velocity SFs behave like multifractals in EIR. Moreover, the circulation around simple loops satisfies the area rule in both the energy inverse cascade and enstrophy forward cascade inertial ranges, which extends the previous idea of area rule for IR of energy forward cascade in 3D turbulence [9,11]. These results have several important implications. That the bifractality is found in both the energy inverse cascade of 2D turbulence and the energy forward cascade of 3D turbulence indicates that this property may be independent of the direction of energy transfer. Our results are, thus, of relevance to geophysical flows where cascades in both directions exist [55]. Moreover, a bifractal circulation is much simpler in terms of analysis and understanding than the multifractal velocity and could lead to a reduction in the complexity of the loop-space reformulation of the Navier-Stokes equations [9,11,45]. That is, the elusive intermittency effect in different types of turbulence, i.e., 3D classical turbulence, quasi-2D classical turbulence, and 3D quantum turbulence, can be manifested more simply by circulation. It may, therefore, serve as a potential theoretical metric for a unified description of turbulence.

---

[*]Corresponding author.
xiakq@sustech.edu.cn

[1] U. Frisch, *Turbulence: The Legacy of A. N. Kolmogorov* (Cambridge University Press, Cambridge, England, 1995), 10.1017/CBO9781139170666.

[2] A. N. Kolmogorov, The local structure of turbulence in incompressible viscous fluid for very large reynolds numbers, Proc. R. Soc. Lond., A: Math. Phys. Sci. **434**, 9 (1991).

[3] R. Benzi, G. Paladin, G. Parisi, and A. Vulpiani, On the multifractal nature of fully developed turbulence and chaotic systems, J. Phys. A **17**, 3521 (1984).

[4] K. R. Sreenivasan and R. Antonia, The phenomenology of small-scale turbulence, Annu. Rev. Fluid Mech. **29**, 435 (1997).

[5] C. Sun, Q. Zhou, and K.-Q. Xia, Cascades of Velocity and Temperature Fluctuations in Buoyancy-Driven Thermal Turbulence, Phys. Rev. Lett. **97**, 144504 (2006).

[6] S. Chen, K. R. Sreenivasan, M. Nelkin, and N. Cao, Refined Similarity Hypothesis for Transverse Structure Functions in Fluid Turbulence, Phys. Rev. Lett. **79**, 2253 (1997).

[7] S. Grossmann, D. Lohse, and A. Reeh, Different intermittency for longitudinal and transversal turbulent fluctuations, Phys. Fluids **9**, 3817 (1997).

[8] K. P. Iyer, K. R. Sreenivasan, and P. Yeung, Scaling exponents saturate in three-dimensional isotropic turbulence, Phys. Rev. Fluids **5**, 054605 (2020).

[9] K. P. Iyer, K. R. Sreenivasan, and P. Yeung, Circulation in High Reynolds Number Isotropic Turbulence is a Bifractal, Phys. Rev. X **9**, 041006 (2019).

[10] K. P. Iyer, S. S. Bharadwaj, and K. R. Sreenivasan, The area rule for circulation in three-dimensional turbulence, Proc. Natl. Acad. Sci. U.S.A. **118**, 1 (2021).

[11] A. A. Migdal, Loop equation and area law in turbulence, Int. J. Mod. Phys. A **09**, 1197 (1994).

[12] N. P. Müller, J. I. Polanco, and G. Krstulovic, Intermittency of Velocity Circulation in Quantum Turbulence, Phys. Rev. X **11**, 011053 (2021).

[13] J. I. Polanco, N. P. Müller, and G. Krstulovic, Vortex clustering, polarisation and circulation intermittency in classical and quantum turbulence, Nat. Commun. **12**, 1 (2021).

[14] C. F. Barenghi, L. Skrbek, and K. R. Sreenivasan, Introduction to quantum turbulence, Proc. Natl. Acad. Sci. U.S.A. **111**, 4647 (2014).

[15] E. Varga, V. Vadakkumbatt, A. J. Shook, P. H. Kim, and J. P. Davis, Observation of Bistable Turbulence in Quasi-Two-Dimensional Superflow, Phys. Rev. Lett. **125**, 025301 (2020).

[16] E. Varga, J. Gao, W. Guo, and L. Skrbek, Intermittency enhancement in quantum turbulence in superfluid He4, Phys. Rev. Fluids **3**, 094601 (2018).

[17] S. P. Johnstone, A. J. Groszek, P. T. Starkey, C. J. Billington, T. P. Simula, and K. Helmerson, Evolution of large-scale flow from turbulence in a two-dimensional superfluid, Science **364**, 1267 (2019).

[18] Yauhen P. Sachkou, C. G. Baker, Glen I. Harris, Oliver R. Stockdale, Stefan Forstner, Matthew T. Reeves, Xin He, David L. Mcauslan, Ashton S. Bradley, Matthew J. Davis, and Warwick P. Bowen, Coherent vortex dynamics in a strongly interacting superfluid on a silicon chip [J], Science **366**, 1480 (2019).

[19] G. Gauthier, M. T. Reeves, X. Yu, A. S. Bradley, M. A. Baker, T. A. Bell, H. Rubinsztein-Dunlop, M. J. Davis, and T. W. Neely, Giant vortex clusters in a two-dimensional quantum fluid, Science **364**, 1264 (2019).

[20] R. H. Kraichnan, Inertial ranges in two-dimensional turbulence, Phys. Fluids **10**, 1417 (1967).

[21] H. Xia, H. Punzmann, G. Falkovich, and M. Shats, Turbulence-Condensate Interaction in Two Dimensions, Phys. Rev. Lett. **101**, 194504 (2008).

[22] G. Boffetta and R. E. Ecke, Two-dimensional turbulence, Annu. Rev. Fluid Mech. **44**, 427 (2012).

[23] J. Paret and P. Tabeling, Intermittency in the two-dimensional inverse cascade of energy: Experimental observations, Phys. Fluids **10**, 3126 (1998).

[24] K. Sreenivasan, A. Juneja, and A. Suri, Scaling Properties of Circulation in Moderate-Reynolds-Number Turbulent Wakes, Phys. Rev. Lett. **75**, 433 (1995).

[25] N. Cao, S. Chen, and K. R. Sreenivasan, Properties of Velocity Circulation in Three-Dimensional Turbulence, Phys. Rev. Lett. **76**, 616 (1996).

[26] Q. Zhou, C. Sun, and K.-Q. Xia, Experimental investigation of homogeneity, isotropy, and circulation of the velocity

field in buoyancy-driven turbulence, J. Fluid Mech. **598,** 361 (2008).

[27] R. Benzi, L. Biferale, M. Struglia, and R. Tripiccione, Self-scaling properties of velocity circulation in shear flows, Phys. Rev. E **55,** 3739 (1997).

[28] See Supplemental Material at http://link.aps.org/supplemental/10.1103/PhysRevLett.130.214001 for more details of the experimental setup, the verification of the two-dimensionality of the flow, and the existence of the two inertial ranges, which includes Refs. [29–38].

[29] H. Xia, M. Shats, and G. Falkovich, Spectrally condensed turbulence in thin layers, Phys. Fluids **21,** 125101 (2009).

[30] A. Babiano, C. Basdevant, and R. Sadourny, Structure functions and dispersion laws in two-dimensional turbulence, J. Atmos. Sci. **42,** 941 (1985).

[31] G. Boffetta and S. Musacchio, Evidence for the double cascade scenario in two-dimensional turbulence, Phys. Rev. E **82,** 016307 (2010).

[32] J. H. Xie and O. Bühler, Exact third-order structure functions for two-dimensional turbulence, J. Fluid Mech. **851,** 672 (2018).

[33] M. K. Rivera, W. B. Daniel, S. Y. Chen, and R. E. Ecke, Energy and Enstrophy Transfer in Decaying Two-Dimensional Turbulence, Phys. Rev. Lett. **90,** 104502 (2003).

[34] Y. Liao and N. T. Ouellette, Spatial structure of spectral transport in two-dimensional flow, J. Fluid Mech. **725,** 281 (2013).

[35] M. Rivera, H. Aluie, and R. Ecke, The direct enstrophy cascade of two-dimensional soap film flows, Phys. Fluids **26,** 055105 (2014).

[36] C. V. Tran and J. C. Bowman, Robustness of the inverse cascade in two-dimensional turbulence, Phys. Rev. E **69,** 036303 (2004).

[37] W. Kramer, G. Keetels, H. Clercx, and G. van Heijst, Structure-function scaling of bounded two-dimensional turbulence, Phys. Rev. E **84,** 026310 (2011).

[38] G. Boffetta, A. Cenedese, S. Espa, and S. Musacchio, Effects of friction on 2d turbulence: An experimental study of the direct cascade, Europhys. Lett. **71,** 590 (2005).

[39] M. K. Rivera and R. E. Ecke, Lagrangian statistics in weakly forced two-dimensional turbulence, Chaos **26,** 013103 (2016).

[40] J. Tithof, B. C. Martell, and D. H. Kelley, Three-dimensionality of one-and two-layer electromagnetically driven thin-layer flows, Phys. Rev. Fluids **3,** 064602 (2018).

[41] Y. Liao, D. H. Kelley, and N. T. Ouellette, Effects of forcing geometry on two-dimensional weak turbulence, Phys. Rev. E **86,** 036306 (2012).

[42] H. Xia, N. Francois, H. Punzmann, and M. Shats, Taylor Particle Dispersion During Transition to Fully Developed Two-Dimensional Turbulence, Phys. Rev. Lett. **112,** 104501 (2014).

[43] J. Paret and P. Tabeling, Experimental Observation of the Two-Dimensional Inverse Energy Cascade, Phys. Rev. Lett. **79,** 4162 (1997).

[44] Z. Zhou, L. Fang, N. T. Ouellette, and H. Xu, Vorticity gradient stretching in the direct enstrophy transfer process of two-dimensional turbulence, Phys. Rev. Fluids **5,** 054602 (2020).

[45] A. Migdal, Universal area law in turbulence, arXiv:1903.08613.

[46] M. Shats, D. Byrne, and H. Xia, Turbulence Decay Rate as a Measure of Flow Dimensionality, Phys. Rev. Lett. **105,** 264501 (2010).

[47] R. A. Akkermans, L. P. Kamp, H. J. Clercx, and G. J. van Heijst, Three-dimensional flow in electromagnetically driven shallow two-layer fluids, Phys. Rev. E **82,** 026314 (2010).

[48] R. Benzi, S. Ciliberto, R. Tripiccione, C. Baudet, F. Massaioli, and S. Succi, Extended self-similarity in turbulent flows, Phys. Rev. E **48,** R29 (1993).

[49] A. Alexakis and L. Biferale, Cascades and transitions in turbulent flows, Phy. Rep. **767,** 1 (2018).

[50] U. Frisch and G. Parisi, Fully developed turbulence and intermittency, Ann. N.Y. Acad. Sci. **357,** 359 (1980).

[51] Z.-S. She and E. Leveque, Universal Scaling Laws in Fully Developed Turbulence, Phys. Rev. Lett. **72,** 336 (1994).

[52] G. Boffetta, A. Celani, and M. Vergassola, Inverse energy cascade in two-dimensional turbulence: Deviations from gaussian behavior, Phys. Rev. E **61,** R29 (2000).

[53] Y. Jun and X. L. Wu, Large-scale intermittency in two-dimensional driven turbulence, Phys. Rev. E **72,** 035302(R) (2005).

[54] R. Cerbus and W. Goldburg, Intermittency in 2d soap film turbulence, Phys. Fluids **25,** 105111 (2013).

[55] D. Balwada, J.-H. Xie, R. Marino, and F. Feraco, Direct observational evidence of an oceanic dual kinetic energy cascade and its seasonality, Sci. Adv. **8,** eabq2566 (2022).